

1 **TEMPORAL EVOLUTION OF**
2 **EXTENSIONAL FAULT-PROPAGATION FOLDS**

3
4 **Christopher Jackson^{1*}, Stephen Corfield², Tom Dreyer¹**

5
6 *¹Norsk Hydro Research Centre, Sandsliveien 90, 5020, Bergen, Norway*

7 *²Corfield Geoscience, 15 Peel Street, Stafford, XXXX XXX, UK*

8
9 **Department of Earth Science & Engineering, Imperial College,*
10 *Prince Consort Road, London, SW7 2BP, UK*

11
12 *Corresponding author: c.jackson@imperial.ac.uk*

13
14 **ABSTRACT**

15 Integration of three-dimensional seismic and well data from the Upper Jurassic North
16 Sea rift provides insights into the temporal evolution of fault-propagation folds in
17 extensional settings. The hangingwall of the Oseberg fault zone is characterised by an
18 asymmetric, fault-parallel syncline interpreted as the hangingwall portion of a
19 breached monocline which formed in response to an upwardly-propagating normal
20 fault. During the early stage of fault-tip propagation, a growth monocline developed at
21 the depositional surface, resulting in early syn-rift units which thinned and onlapped
22 towards the fault zone. Stratigraphic data from these early syn-rift units suggest that
23 this initial phase of growth folding lasted *ca.* 19 Myr. Late syn-rift units formed an
24 overall faultward expanding wedge, suggesting it was deposited after monocline
25 breaching and a more typical half-graben basin had established. The results of this
26 study have important implications for the timescale over which fault-propagation
27 folds evolve prior to breaching and the impact of fault-propagation folding on the
28 sequence stratigraphy of syn-rift successions.

29
30 **Keywords:** rift-basin, fault-propagation folding, normal faults, syn-rift

31
32 **INTRODUCTION**

33 Physical analogue (e.g. Withjack et al. 1990; Withjack & Callaway, 2000) and
34 numerical (e.g. Allmendinger, 1998; Hardy & McClay, 1999; Finch et al. 2004)

35 modelling, in combination with outcrop (e.g. Gawthorpe et al. 1997; Sharp et al.
36 2000; Jackson et al. 2006) and subsurface studies (e.g. Corfield & Sharp, 2000;
37 Maurin & Niviere, 2000) have demonstrated that fault-propagation folding is an
38 important process during the early stages of fault growth in rift basins. In addition,
39 fault-propagation folding not only controls the geometry of the basin margin through
40 time, but it can also strongly influence the architecture and sequence stratigraphy of
41 coeval syn-rift successions (e.g. Gawthorpe et al. 1997). Despite its obvious
42 importance in the structural and stratigraphic development of rift basins, the evolution
43 of fault-propagation folds and their impact on the sequence stratigraphy of syn-rift
44 successions remains poorly understood. This stems from the fact that physical
45 analogue and numerical models can predict the geometric and kinematic evolution of
46 extensional fault-propagation folds, but cannot explicitly model over what timescales
47 such structures develop in nature (e.g. Withjack et al. 1990; Hardy & McClay, 1999;
48 Finch et al. 2004). Furthermore, lack of age-constrained growth strata preserved
49 adjacent to fault-propagation folds at outcrop means it is often not possible to
50 accurately document the temporal evolution of the structures (e.g. Khahil & McClay,
51 2002; Keller & Lynch 2000) or to determine their impact on the geometry and
52 sequence stratigraphic variability on coeval syn-rift units.

53 Integration of three-dimensional seismic data and well data provides one
54 method for documenting the temporal evolution of fault-propagation folds and their
55 influence on syn-rift stratigraphy (e.g. see approach utilised by Corfield & Sharp,
56 2000 and Maurin & Niviere, 2000). Modern three-dimensional seismic data allows
57 the geometry and scale of rift-related faults, folds and associated syn-rift stratigraphy
58 to be accurately determined, whereas well data integrated with biostratigraphic dating
59 of recognised key stratal surfaces allows analysis of the syn-rift sequence stratigraphic
60 variability and dating of the structural development. We present the results of a
61 subsurface analysis of a rift-related normal fault and associated fault-propagation fold
62 from the Upper Jurassic of the North Sea rift basin. The results of this study have
63 important implications for the temporal evolution of fault-propagation folds in rift
64 basins and the sequence stratigraphic variability of the associated syn-rift succession.

65

66 **REGIONAL STRUCTURAL SETTING AND STRATIGRAPHIC** 67 **FRAMEWORK**

68 The study area is located on the Horda Platform along the eastern margin of
69 the North Sea rift basin approximately 200 km offshore Norway (Fig. 1). The North
70 Sea rift basin formed in response to crustal extension during the Late Jurassic which
71 formed a series of fault-blocks bounded by dominantly N-S trending normal faults.
72 The Oseberg fault, which forms the focus of this study, is interpreted to have become
73 active in the Early Bathonian and may have involved reactivation of an earlier,
74 basement-involved normal fault related to the preceding Permo-Triassic rift event
75 (Faerseth & Ravnås, 1998). Regional studies suggest that this area of the North Sea
76 rift basin did not undergo compression during the Late Jurassic post-rift period (Fraser
77 et al 2003).

78 The Brent Group was deposited in a marginal to shallow marine environment
79 (e.g. Mitchener et al. 1992) and is typically interpreted to represent a pre-rift unit
80 deposited prior to the Late Jurassic rift event. Several studies have suggested however
81 that the upper part of the unit may have been deposited during the earliest stage of
82 rifting (Ravnås & Steel, 1997; Davies et al. 2000). The Brent Group (SU1; Figs 2, 3
83 and 4) is conformably overlain across a flooding surface dated at 171 Ma by a
84 transgressive syn-rift interval which can be divided into two units. The lower, early
85 syn-rift unit (SU2; Figs 2, 3 and 4) comprises shallow marine sandstones and shelfal
86 siltstones and mudstones which are separated by a flooding surface. Within the shelfal
87 succession an erosional unconformity dated to span 158-161 Ma is developed. The
88 overlying, late syn-rift unit (SU3; Figs 2, 3 and 4) which comprises a deep marine
89 succession overlies the early syn-rift unit across a composite unconformity/flooding
90 surface which spans 152-154 Ma. The top of the syn-rift interval is defined by a
91 regional flooding surface which marks the end of the rift event. Additional wireline
92 and biostratigraphic analysis permits recognition of additional key stratal surfaces and
93 allows both the early and late syn-rift units to be internally subdivided (Fig. 4).

94

95 **GENERAL STRUCTURAL STYLE OF THE OSEBERG FAULT**

96 The Oseberg fault is planar, strikes N-S, dips steeply ($>60^\circ$) to the west, and
97 has a maximum displacement of 175 m (Fig. 2). The hangingwall of the Oseberg fault
98 is characterised by an asymmetric, fault-parallel syncline, the axis of which is located
99 1.6 km westwards of the fault zone. The hangingwall syncline is up to 4.2 km wide
100 and consists of a steeply-dipping (14°) eastern limb located in the immediate
101 hangingwall of the Oseberg fault, and a more gently-dipping (2°) opposing limb. A

102 series of moderate displacement (50-70 m) normal faults splay out from the Oseberg
103 fault into its hangingwall of the Oseberg fault. The footwall of the Oseberg fault is
104 poorly-imaged, but units dip either gently westwards towards or gently eastward away
105 from the fault zone. Although this fault-related fold shares many similar geometrical
106 characteristics to fault-propagation folds described from other extensional settings
107 (e.g. Withjack et al. 1990; Gawthorpe et al. 1997; Pascoe et al. 1999; Maurin &
108 Niviere, 2000), the stratal architecture of the associated syn-rift units must be
109 considered before an interpretation of its origin can be proposed.

110

111 **SYN-RIFT STRATAL ARCHITECTURE**

112 Seismic and well data are integrated to analyse the stratal architecture of the
113 syn-rift basinfill as a tool to determine the origin of the fault-related fold described
114 above. In both data types, focus is placed on syn-rift thickness variations and onlap
115 relationships, observed both within and between stratal units, and in both map-view
116 and cross-section. Three stratal units can be mapped on three-dimensional seismic
117 data in the hangingwall of the Oseberg fault (SU1-3; Figs. 2-4). Based on correlation
118 to well data it is demonstrated that SU1 corresponds to the upper pre-rift unit (169-
119 171 Ma), SU2 corresponds to the lower syn-rift unit (151-169 Ma) and SU3
120 corresponds to the upper syn-rift unit (144-151 Ma) (Fig. X). Although seismic data
121 allows documentation of the large-scale stratal architecture, the vertical resolution is
122 insufficient to resolve the distribution of the six small-scale stratal units developed in
123 the syn-rift succession. The distribution of these units is analysed using data from the
124 three wells which penetrate the hangingwall syn-rift interval (Fig. 4).

125

126 **Stratal Unit 1 (SU1 – 169-171 Ma)**

127 Stratal Unit 1 (SU1) is deformed by the fault-parallel fold described above but
128 displays no systematic dip or strike-orientated changes in thickness with respect to the
129 Oseberg fault or associated fold (Fig. 2). This observation is confirmed by well data
130 which indicates that the unit is broadly tabular across the majority of the half-graben,
131 being 52 m in the axis of the hangingwall syncline and thinning to 39 m in the
132 immediate hangingwall of the Oseberg fault due to erosion beneath overlying units
133 (SU1; Fig. 4). Well data indicates that a flooding surface identified within SU1 is
134 conformable to the top and base of the unit and can be mapped across the entire width
135 of the Omega terrace.

136

137 **Stratal Unit 2 (SU2 – 151-169 Ma)**

138 In contrast to SU1, SU2 displays marked variations in thickness with respect
139 to the Oseberg fault and its associated fold. Seismic mapping indicates that SU2
140 thickens eastwards down the hangingwall dipslope and is thickest in the axis of the
141 Omega terrace, but thins eastwards into the immediate hangingwall of the Oseberg
142 fault (Fig. 3A). Thinning of SU2 towards the Oseberg fault is accommodated by onlap
143 of the lowermost seismic reflections onto the steep-dipping, west-facing limb of the
144 hangingwall syncline defined by the top of SU1 (Fig. 2A).

145 Well data supports the seismic observation that SU2 is thickest in the axis of
146 the hangingwall syncline, 1.6 km westwards of the Oseberg fault, and thins towards
147 and is absent in the immediate hangingwall of the Oseberg fault (Fig. 4). Additionally,
148 well data suggests that eastwards thinning of SU2 is achieved by a combination of
149 onlap onto underlying units (which dip at a shallower angle; Fig. 4) and low-angle
150 truncation beneath overlying units, with key stratal surfaces within SU2 merging
151 towards the fault onto the steep-dipping limb of the hangingwall syncline (Fig. 4). As
152 a result, in the immediate hangingwall of the fault a composite key stratal surface is
153 developed such that the upper syn-rift unit (SU3) directly overlies the uppermost pre-
154 rift unit (SU1) and the early syn-rift unit (SU2) is absent (Fig. 4).

155

156 **Stratal Unit 3 (SU3 – 144-151 Ma)**

157 Seismic data indicates that along the Oseberg fault zone SU3 either has a
158 wedge-shaped geometry and thickens eastwards into the immediate hangingwall of
159 the fault or a more tabular geometry and is broadly equal thickness across the fault
160 block (Fig. 3B). Where a wedge-shaped geometry is observed, westwards thinning of
161 SU3 up the hangingwall dipslope appears to be accommodated by onlap onto the
162 seismic reflection bounding the top of the underlying SU2 (Fig. 2).

163 On the correlation panel shown in Fig. 4, SU3 is broadly tabular and is
164 thickest 3.8 km westwards of the Oseberg fault (Fig. 4). SU3 onlaps and oversteps
165 SU2 eastwards towards the Oseberg fault, and in contrast to the underlying unit is
166 developed in the immediate hangingwall of the fault where it directly overlies the
167 uppermost pre-rift unit (SU1) (Fig. 4). Key stratal surfaces within SU3, in contrast to
168 those developed in the underlying SU2, are approximately parallel with the top and
169 base of the unit and do not converge eastwards towards the Oseberg fault. Dips within

170 SU3 are overall quite gentle ($<1^\circ$; Fig. 4) across the width of the Omega terrace and
171 are typically less than observed in the underlying units.

172

173 **ORIGIN AND EVOLUTION OF THE OSEBERG FAULT AND FAULT-** 174 **RELATED FOLD**

175 Three potential models can be proposed for the development of the Oseberg
176 fault and the related fault-parallel fold. Firstly, the fold may have originated in
177 response to post-rift compression of the hangingwall (cf. Knott, 2001), although this
178 model is rejected due to the observation that the spatial variability of the syn-rift
179 succession clearly indicates that structural growth occurred during the syn-rift, and the
180 lack of regional data suggesting post-rift compression occurred in this part of the
181 North Sea rift. Differential compaction is also not considered to be a viable
182 mechanisms for fold development as structural growth related to this mechanism
183 would have had to have been almost instantaneous between the pre and syn-rift stages
184 (i.e. post-SU1 and pre-SU1) and, therefore, would have needed to have occurred in
185 the absence of significant loading by the syn-rift succession. Finally, frictional drag
186 adjacent to the fault is also rejected as a viable mechanism for the formation of the
187 fault-related fold, as such drag folds are typically an order of magnitude narrower (i.e.
188 10-100's of metres) than the fold described here.

189 Based on the scale of the fold and the architecture of the associated syn-rift
190 succession, our preferred model for the origin of the fault-related fold in the
191 hangingwall of the Oseberg fault is as a fault-propagation fold which initially
192 developed above an upwardly-propagating fault. Based on the architecture and dating
193 of the syn-rift succession, temporal constraints can be placed on the onset, duration
194 and cessation of fault-propagation folding. During deposition of SU1, the Oseberg
195 fault is interpreted to have been inactive as suggested by the tabular geometry of this
196 unit across the width of the hangingwall (Fig. 5). It should be noted that the fault may
197 have been active at depth but did not influence at-surface topography or the resultant
198 syn-rift architecture. At-surface growth folding began at 169 Ma at the start of
199 deposition of SU2 as indicated by thinning and onlap of this unit towards the fault
200 onto the steep, westwards-dipping limb of the hangingwall syncline. The site of
201 maximum subsidence and hence sediment accumulation was located in the synclinal,
202 fault-parallel depocentre offset 2.8 km from future position of the Oseberg fault (SU2;
203 Figs. 2, 3 & 5). Incremental fault slip, fold amplification and rotation of previously

204 deposited syn-rift units resulted in the formation of progressive unconformities (see
205 discussion below) whereby successive key stratal surfaces (flooding surface and
206 erosional surfaces) surfaces merge towards the growing structure. Similar geometries
207 have been documented adjacent to growing structures in both extensional (e.g. Maurin
208 & Niviere, 2000) and compressional structures (e.g. Ford et al. 1997; Gawthorpe et al.
209 2000).

210 In contrast to SU2, the late syn-rift unit (SU3) thickens towards the Oseberg
211 fault, suggesting that the fault had breached the fault-propagation fold and from 151
212 Ma onwards was a surface-breaking feature (Fig. 5). Breaching of the fault-
213 propagation fold, possibly augmented by uplift in the footwall to the fault bounding
214 the western margin of the fault block, resulted in eastwards rotation of the
215 hangingwall dip slope as indicated by westwards onlap of SU2 onto the hangingwall
216 dip slope (Fig. 5). This change in structural style was associated with a migration in
217 the locus of maximum subsidence and sediment accumulation eastwards towards the
218 immediate hangingwall of the Oseberg fault (Fig. 5). Thinning of the late syn-rift unit
219 along portions of the Oseberg fault (e.g. Fig. 4) suggests that although the fault-
220 propagation fold had been breached, the steep-dipping limb of the hangingwall
221 syncline locally still had a topographic expression in the hangingwall of the fault. The
222 Oseberg fault persisted as a surface-breaking feature until the end of rifting at 144
223 Ma.

224

225 **DISCUSSION**

226 Our study places broad temporal constraints on the potential duration of fault-
227 propagation folding during normal fault growth, and suggests that in the present study
228 area at-surface growth folding characterised the initial *ca.* 19 My of activity on the
229 Oseberg fault before the fold was fully breached along its length. The Revfallet fault,
230 offshore Mid-Norway (Pascoe et al. 1999; Corfield & Sharp, 2000) and the western
231 margin of the Rhine Graben (Maurin & Niviere, 2000) are two areas where the
232 temporal evolution of fault-propagation folding has also been resolved using the
233 coeval syn-rift architecture. Fault-propagation folding along the Revfallet fault was
234 ongoing for *ca.* 24 Myr and the fold was only locally breached, whereas in the Rhine
235 Graben the duration of the fault-propagation folding prior to fold breaching can be
236 dated to have lasted *ca.* 3.5 Myr. The marked variability in the duration of fault-
237 propagation folding demonstrated by these examples and the present study may

238 reflect the rate at which the basin-bounding fault propagates, the strength of the cover
239 stratigraphy or the degree of coupling of faulting at depth and folding in the cover as
240 suggested by physical analogue (e.g. Withjack et al. 1990; Withjack & Callaway,
241 2000) and numerical models (e.g. Hardy & McClay, 1999; Finch et al. 2004). For
242 example, along the Revfallet fault a thick evaporite horizon at the base of the
243 sedimentary cover sequence inhibited the upward propagation of the basin-bounding
244 fault, hence (i) the relative longevity of fault-propagation folding (e.g. *ca.* 24 Myr)
245 and (ii) only local breaching of the fault-propagation fold along-strike (cf. Withjack &
246 Callaway, 2000). In contrast, the relatively short duration of fault-propagation folding
247 indicated by the Rhine Graben example may reflect the rapid upward propagation of
248 the fault through a brittle carbonate-dominated cover sequence containing only thin
249 evaporite-rich horizons.

250 Fault-propagation folding also markedly affected the stratigraphic
251 development of the syn-rift basinfill. In addition to controlling the large-scale
252 architecture of the syn-rift succession, fault-propagation folding also strongly
253 influenced the spatial development of key stratal surfaces within the syn-rift. For
254 example, syn-rift unconformities become increasingly erosional towards the crest of the
255 fault-propagation fold and accordingly represent increasingly larger periods of time
256 and missing strata. Conversely, the unconformities become suppressed in the
257 hangingwall syncline where subsidence and hence accommodation was greater (e.g.
258 within SU2; Fig. 4). One consequence of unconformities becoming enhanced towards
259 the evolving fault-propagation fold is that marine flooding surfaces during the early
260 syn-rift are restricted to the hangingwall syncline axis due to later erosion beneath
261 syn-rift unconformities. Only during the late syn-rift when subsidence and
262 accommodation is greater in the immediate hangingwall do marine flooding surfaces
263 become more areally widespread. Clearly such temporal and spatial variability of key
264 stratal surface development has major implications for correlating such surfaces over
265 relatively short (i.e. 1-3 km) length-scales (cf. Gawthorpe et al. 1997; 2000).

266

267 **ACKNOWLEDGMENTS**

268 Rob Gawthorpe, Mike Young and Mark Scott are thanked for discussions during this
269 study. Norsk Hydro and partners within licence XXX are thanked for permission to
270 publish the results of this study.

271

272 **REFERENCES**

273

274 Allmendinger, R.W., 1998, Inverse and forward numerical modelling of tri-shear
275 fault-propagation folds: *Tectonics*, v. 17, p. 62-81.

276

277 Corfield, S.C., and Sharp, I.R., 2000, Structural style and stratigraphic architecture of
278 fault propagation folding in extensional settings: a seismic example from the
279 Smørbukk area, Halten Terrace, Mid-Norway: *Basin Research*, v. 12, p. 329-
280 341.

281

282 Davies, S.J., Dawers, N.H., McLeod, A.E., and Underhill, J.R., 2000, The structural
283 and sedimentological evolution of early syn-rift successions: the Middle
284 Jurassic Tarbert Formation, North Sea: *Basin Research*, v. 12, p. 343-365.

285

286 Finch, E., Hardy, S., and Gawthorpe, R.L., 2004, Discrete-element modelling of
287 extensional fault-propagation folding above rigid basement fault blocks: *Basin*
288 *Research*, v. 16, p. 467-488.

289

290 Ford, M., Williams, E.A., Artoni, A., Verges, J., and Hardy, S., 1997, Progressive
291 evolution of a fault-related fold pair from growth strata geometries, Sant
292 Llorenç de Morunys, SE Pyrenees: *Journal of Structural Geology*, v. 19, p. 413-
293 441.

294

295 Færseth, R. B., and Ravnås, R., 1998, Evolution of the Oseberg fault block in context
296 of the northern North Sea structural framework: *Marine and Petroleum*
297 *Geology*, v. 15, p. 467-490.

298

299 Gawthorpe, R.L., Sharp, I.R., Underhill, J.R., and Gupta, S., 1997, Linked sequence
300 stratigraphic and structural evolution of propagating normal faults: *Geology*, v.
301 25, p. 795-798.

302

303 Gawthorpe, R.L., Hall, M., Sharp, I.R., and Dreyer, T., 2000, Tectonically enhanced
304 forced regressions: examples from growth folds in extensional and
305 compressional settings, the Miocene of the Suez Rift and the Eocene of the

306 Pyrenees, *in* Hunt, D., and Gawthorpe, R.L., eds., Sedimentary responses to
307 forced regressions: Geological Society (London) Special Publication 172, p.
308 177-192.
309

310 Hardy, S., and McClay, K., 1999, Kinematic modelling of extensional fault-
311 propagation folding: *Journal of Structural Geology*, v. 21, p. 695-702.
312

313 Jackson, C.A.L., Gawthorpe, R.L., and Sharp, I.R., 2006, Style and sequence of
314 deformation during extensional fault-propagation folding: examples from the
315 Hammam Faraun and El-Qaa fault blocks, Suez Rift, Egypt: *Journal of*
316 *Structural geology*, v. 28, p. 519-535.
317

318 Keller, J.V.A., and Lynch, G., 2000, Displacement transfer and forced folding in the
319 Maritimes basin of Nova Scotia, eastern Canada, *in* Cosgrove, J.W., and
320 Ameen, M.S., eds., *Forced folds and fractures: Geological Society (London)*
321 *Special Publication 169*, p. 87-101.
322

323 Khalil, S.M., and McClay, K.R., 2002, Extensional fault-related folding, northwestern
324 Red Sea, Egypt: *Journal of Structural Geology*, v. 24, p. 743-762.
325

326 Knott, S.D., 2001, Gravity-driven crustal shortening in failed rifts: *Journal of the*
327 *Geological Society of London*, v. 158, p. 193-196.
328

329 Maurin, J-C., and Niviere, B., 2000, Extensional forced folding and décollement of
330 the pre-rift series along the Rhine Graben and their influence on the geometry of
331 the syn-rift sequences, *in* Cosgrove, J.W., and Ameen, M.S., eds., *Forced folds*
332 *and fractures: Geological Society (London) Special Publication 169*, p. 73-86.
333

334 Mitchener, B.C., Lawrence, D.A., Partington, M.A., Bowman, M.B.J., and Gluyas, J.,
335 1992, Brent Group: sequence stratigraphy and regional implications, *in* Morton,
336 A.C., Haszeldine, R.S., Giles, M.R., and Brown, S., eds., *Geology of the Brent*
337 *Group: Geological Society (London) Special Publication 61*, p. 45-80.
338

- 339 Pascoe, R., Hooper, R., Storhaug, K., and Harper, H., 1999, Evolution of extensional
340 styles at the southern termination of the Nordland Ridge, mid-Norway: a
341 response to variations in coupling above Triassic salt, *in* Fleet, A.J., and Boldy,
342 S.A.R., eds., *Petroleum Geology of Northwest Europe Proceedings of the 5th*
343 *Conference*, pp. 83-90.
344
- 345 Ravnås, R., and Steel, R.J., 1997, Contrasting styles of Late Jurassic syn-rift turbidite
346 sedimentation: a comparative study of the Magnus and Oseberg areas, northern
347 North Sea: *Marine and Petroleum Geology*, v. 14, p. 417-449.
348
- 349 Sharp, I.R., Gawthorpe, R.L., Underhill, J.R., and Gupta, S., 2000, Fault propagation
350 folding in extensional settings: examples of structural style and syn-rift
351 sedimentary response from the Suez Rift, Egypt: *Geological Society of America*
352 *Bulletin*, v. 112, p. 1877-1899.
353
- 354 Withjack, M.O., Olson, J., and Peterson, E., 1990, Physical models of extensional
355 forced folds: *American Association of Petroleum Geologists Bulletin*, v. 74, p.
356 1038-1054.
357
- 358 Withjack, M.O., and Callaway, S., 2000, Active normal faulting beneath a salt-layer:
359 physical study of deformation patterns in the cover sequence: *American*
360 *Association of Petroleum Geologists*, v. 84, p. 627-651.
361

362 **FIGURE CAPTIONS**

363

364 Figure 1. Map indicating the location of the study area in the North Sea. The locations
365 of wells used in this study and Fig. 3 are also shown.
366

367 Figure 2. Representative (time-migrated) seismic section across the Omega Terrace
368 flattened on the top of SU3 (top syn-rift) indicating the geometry of the fault-
369 propagation fold and associated stratal units. Location of seismic section is shown in
370 Fig. 3. Seismic horizons which were mapped and used to construct Figs. 3A and 3B
371 are marked. Black represents a downward increase in acoustic impedance and data is
372 zero-phase.

373

374 Figure 3. A: Seismic isochron map of SU2. B: Seismic isochron map of SU3. Scale is
375 in millisecond (ms) two-way traveltime (TWTT). Locations of Figs. 2 and 4 are
376 shown.

377

378 Figure 4. Well-based correlation across the eastern part of the Omega terrace
379 illustrating the architecture of stratal units associated with the fault-propagation fold.
380 Locations of wells used are shown in Fig. 3. GR = gamma-ray and scale is from 0
381 (left) to 150 (right) API. Ages of selected key stratal surfaces are shown.

382

383 Figure 5. Schematic reconstruction indicating the evolution of the fault-propagation
384 fold and variability in stratal architecture and key stratal surface development. A:
385 Early syn-rift – SU2 (151-169 Ma). B: Late syn-rift – SU3 (144-151 Ma). See text for
386 full discussion. Key to stratigraphic units and key stratal surfaces is the same as in
387 Fig. 4. Note that details of key stratal surface development are only shown for the
388 interval considered.

Fig. 1

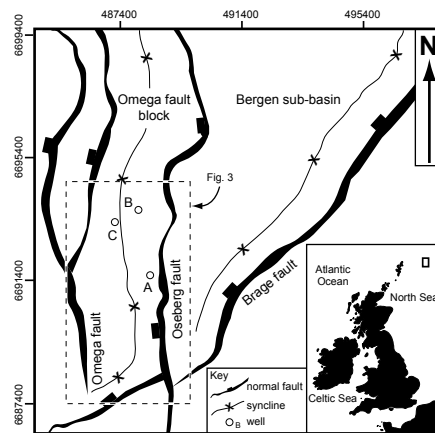


Figure 1. Map indicating the location of the study area in the North Sea. The locations of wells used in this study and Fig. 3 are also shown.

Fig. 2

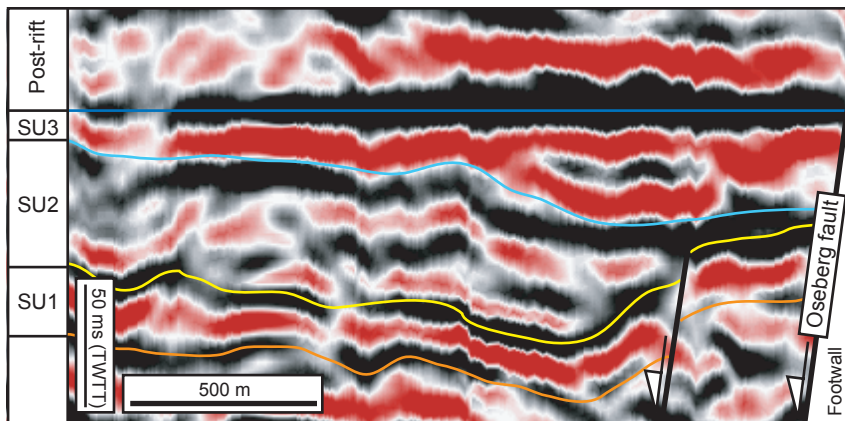


Figure 2. Representative (time-migrated) seismic section across the Omega Terrace flattened on the top of SU3 (top syn-rift) indicating the geometry of the fault-propagation fold and associated stratal units. Location of seismic section is shown in Fig. 3. Seismic horizons which were mapped and used to construct Figs. 3A and 3B are marked. Black represents a downward increase in acoustic impedance and seismic data is zero-phase. Note the minor fault developed in the hangingwall of the Oseberg fault.

Fig. 3

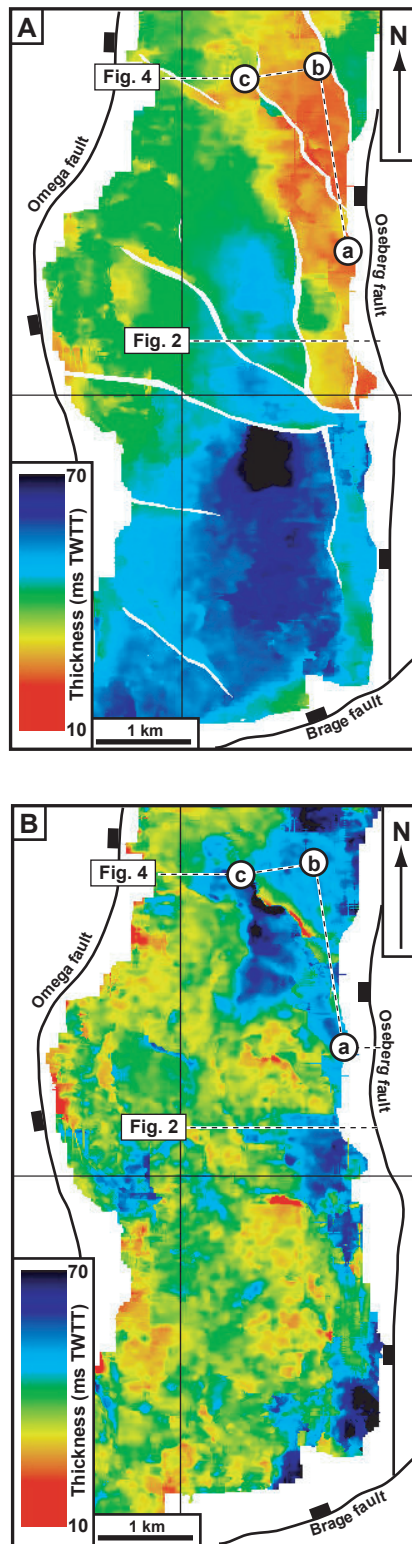


Figure 3. A: Seismic isochron map of SU2. B: Seismic isochron map of SU3. Scale is in millisecond (ms) two-way traveltime (TWTT). Locations of Figs. 2 and 4 are shown.

Fig. 4

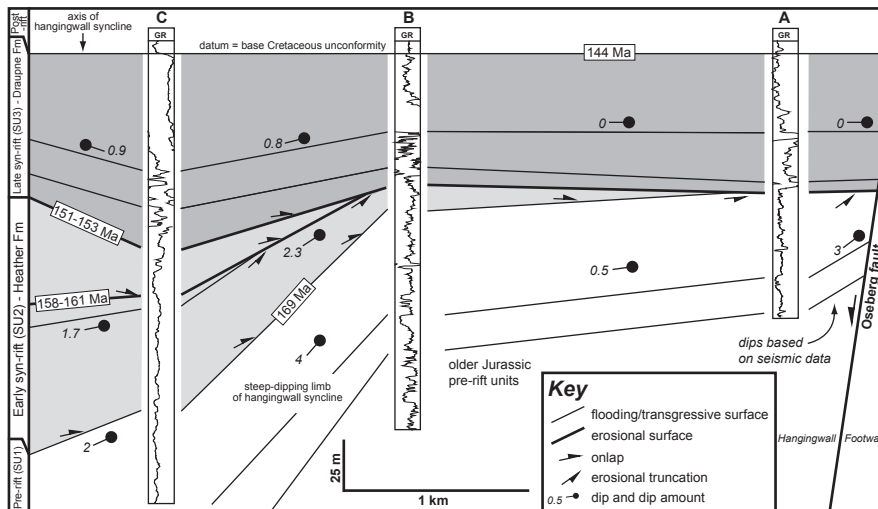


Figure 4. Well-based correlation across the eastern part of the Omega terrace illustrating the architecture of stratal units associated with the fault-propagation fold. Locations of wells used are shown in Fig. 3. GR = gamma-ray and scale is from 0 (left) to 150 (right) API. Ages of selected key stratal surfaces are shown.

Fig. 5

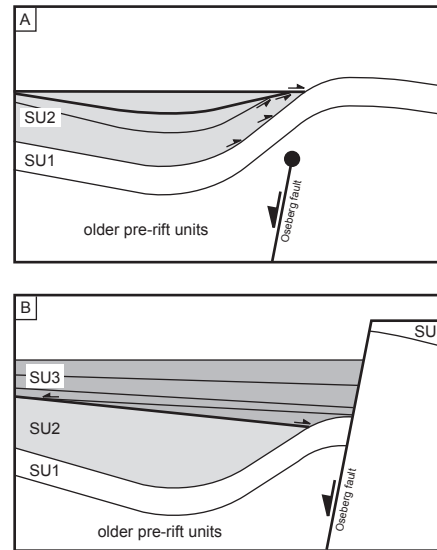


Figure 5. Schematic reconstruction indicating the evolution of the fault-propagation fold and variability in stratal architecture and key stratal surface development. A: Early syn-rift – SU2 (151-169 Ma). B: Late syn-rift – SU3 (144-151 Ma). See text for full discussion. Key to stratigraphic units and key stratal surfaces is the same as in Fig. 4. Note that details of key stratal surface development are only shown for the interval considered and only the main Oseberg fault is shown for clarity.